High magnetization FeCo nanoparticles for magnetorheological fluids with enhanced response

Virginia Vadillo [a) *], Ainara Gómez [b)], Joanes Berasategi [b)], Jon Gutiérrez [a,c)], Maite Insausti [a,c)], Izaskun Gil de Muro [a,c)], Joseba S. Garitaonandia [a,c)], Arantxa Arbe [d)], Amaia Iturrospe [d)], M. Mounir Bou-Ali [b)] and Jose Manuel Barandiarán [c)]

Abstract

We present results concerning the fabrication of a new magnetorheological fluid with FeCo magnetic nanoparticles (NPs) as magnetic fillers. These NPs have been fabricated by using the chemical reduction technique and show a pure crystalline phase with size ranging among 30-50 nm and high magnetization, 212 ± 2 Am^2/kg. They agglomerate due to the strong magnetic dipolar interaction among them.

These FeCo nanoparticles were used to synthesize a magnetorheological fluid by using oleic acid as surfactant, mineral oil as carrier liquid and Aerosil 300 as additive to control the viscosity of the fluid. The synthesized fluid showed a strong magnetorheological response with increasing shear stress values as the magnetic field intensity increases. Thus, we have measured a superior performance up to 616.7 kA/m, with a yield stress value of 2729 Pa, and good reversibility after demagnetization process. This value competes with the best ones reported in the most recent literature. We have compared the obtained results with our previous reported ones by using high magnetization Fe NPs fabricated by the electrical explosion of wire method (Fe-EEW).

Keywords: Iron Cobalt alloy, magnetic nanoparticles, magnetic properties, magnetorheological fluid, magnetorheological behaviour

a) BCMaterials (Basque Center for Materials, Applications & Nanostructures), UPV/EHU Scientific Park, Bldg. Martina Casiano, 3rd. Floor, Barrio Sarriena s/n, 48940, Leioa, Spain.
b) Mechanical and Industrial Production Department, Faculty of Engineering, Mondragon Unibersitatea, Loramendi 4, E-20500 Arrasate-Mondragón, Spain
c) Faculty of Science and Technology, University of the Basque Country UPV/EHU, P. Box 644, 48080 Bilbao, Spain.
d) Centro de Física de Materiales (CFM) (CSIC–UPV/EHU)—Materials Physics Center (MPC), Paseo Manuel de Lardizabal 5, 20018 Donostia-San Sebastián, Spain.

** Corresponding author: Virginia Vadillo*
email: virginia.vadillo@bcmaterials.net

1. Introduction

Magnetorheological (MR) fluids are stable suspensions of magnetic particles in a carrying fluid. One of their most important characteristics is the reversible rheological behaviour they exhibit, that can be modified by application of an external magnetic field. Because of this, they are also called "intelligent" fluids. As a first consequence, the behaviour of MR fluids can be adapted to variable working conditions.[1-3] A first classification of the magnetic fluids follows the particle size criterion. Thus, according to Charles the magnetic fluids can be classified in two main groups[4]: ferrofluids (FF) composed by nanometric magnetic particles (MNPs) and magnetorheological (MR) fluids with dispersed micron-size particles. Nevertheless, this criterion is diffuse since MR fluids have been already synthesized with very small iron MNPs of the order of 20 nm and 30 nm, [5,6] or with quite large iron particles of the order of 1000 nm. Those are much boarder size limits as compared with the previous classification.[7]

Deeping in the previous classification of the magnetic fluids, magnetorheological (MR) fluids can be defined as composed of magnetic microparticles, that is, magnetic multidomain particles, dispersed in a liquid carrier. They display the characteristics of MR fluids: In absence of applied magnetic field, there is no magnetic interaction among them and the observed MR behaviour is that of a suspension of non-interacting particles, that is Newtonian-type, provided the particle concentration is far from the maximum packing fraction. However, under the application of an external magnetic field, a net magnetic moment arises in the magnetic fillers, and the attractive magnetostatic interaction among them gives rise to the formation of chain-like structures directed along the direction of the applied field. This result in a very fast transition from a liquid to almost solid state in which a finite stress (the yield stress) is needed to break the chain-like structures of the magnetic fillers. It has been already demonstrated that this field induced stress rises quadratically with the saturation magnetization of the magnetic filler.[8] The maximum field value of the yield stress will happen when the aligned particles become magnetically saturated. As a direct consequence, the flow of the fluid is hindered and the rheological behaviour changes to that of a plastic material, exhibiting big changes in its viscosity and high values of that yield stress.[9,10]

On the other hand, the ferrofluid rigorous definition concerns a colloidal suspension of nanoparticles of ferro- or ferrimagnetic materials dispersed in a liquid carrier.[4] This FF does not settle out under an external field action (gravitational or magnetic)[11], a fact which restricts the size of the magnetic filler to be smaller to 10 nm in

diameter and coated with some dispersant agent that prevents the action of van der Waals attractive forces. In this case, Brownian motion overcomes other types of interactions. The effect of a magnetic field in the rheological properties is just a slight increase of the FF viscosity, due to a small rotation of the nanoparticles within the fluid, because of the tendency of magnetic moments to align with that applied field. However, there is no appearance of any yield stress.[12,13] Nevertheless, in real ferrofluids even low magnetization particles can be size distributed or they just aggregate within the carrier fluid, so that the dipole-dipole interaction can overcome Brownian motion and give rise to high changes in their viscosities as well as the appearance of a yield stress. This is for instance the case of nanofluids made with iron oxide nanoparticles[14] or bio-ferrofluids made with multi-core iron oxide nanoparticles that show yield stress and Herschel-Bulkley behaviour accompanied by a great increase of the effective viscosity under applied magnetic field.[15]

Much more appropriate than focusing exclusively in the magnetic filler size, is to use the interaction parameter λ, which compares the magnetostatic energy of the dipole-dipole interaction ($\propto a^3\langle M_p^2\rangle$, where a is the magnetic filler radius and $\langle M_p\rangle$ is the mean magnetization of the particle) with the thermal energy ($\propto k_B T$, where k_B is the Boltzmann constant and T is the absolute temperature).[3,11,16] For single core dispersed particles, λ is given by:

$$\lambda = \frac{\pi \mu_0 \mu_{cr} a^3 \langle M_p^2 \rangle}{18 k_B T} \tag{1}$$

In this expression μ_0 and μ_{cr} are the permeabilities of vacuum and the liquid carrier ($\mu_{cr} \approx 1$ for water), respectively. Now we can distinguish ferrofluids, with $\lambda < 1$, from MR fluids, in which λ is field dependent and $\lambda >> 1$ even in moderate magnetic fields. The frontier between FF and MRF (or mono- and multidomain magnetic filler containing fluids) corresponds to $\lambda \approx 1$.[16]

When fluid suspensions contain dispersed particles or even aggregates of these particles, both an interaction parameter[10] and the surfactant layer preventing direct contact of the particles[17] have to be taking into account, leading to a magnetic field dependent parameter λ:

$$\lambda = \frac{\pi \mu_0 \mu_{cr} \beta^2 a^3 H_0^2}{2 k_B T} \left(\frac{a}{a+s}\right)^3 \tag{2}$$

with

$$\beta = \frac{\mu_p - \mu_{cr}}{\mu_p + 2\mu_{cr}} \quad (3)$$

where μ_p is the magnetic particle permeability, s is the surfactant thickness and H_0 the applied magnetic field intensity. The parameter β is known as the magnetic contrast factor. In the case of magnetic fillers with high permeability, as compared with the carrier liquid, $\beta \approx 1$.[15]

Colloidal stability of the magnetic fluids is also a critical parameter for the good performance of any MR device.[2] Since ferrofluids have usually MNPs as magnetic filler, they intrinsically present good stability as the Brownian effect is sufficient to prevent the particle's sedimentation.[4] On the other hand, the MR fluids present the intrinsic problem of particle sedimentation due to their size.[18] There are several strategies to prevent aggregation and minimize sedimentation of the magnetic fillers like the use of viscoplastic carriers (such as greases), the use of core-shell type particles, bi-disperse like systems, etc. Among these, one of the most actually used to reduce particles aggregation and sedimentation is a stabilizing agent. Despite the big effort carried out in recent years analysing different agent compositions for enhanced MR fluids stability this problem still remains.[10,19-21]

The idea to use iron particles due to their high saturation magnetization value and consequently increase the MR performance of the fabricated fluid is not new).[22] Thus, in a previous work,[23] the authors studied the behaviour of two magnetorheological fluids fabricated with two different types of magnetic particles as fillers: pure Fe nanoparticles obtained by the Electric Explosion of the Wire (EEW) technique, 77 ± 3 nm size with high saturation magnetization value of 190 Am^2/kg, and commercial CIP (Carbonyl Iron Powder, BASF, Germany) microsized particles, 1 ± 0.4 μm with saturation magnetization value of 177 Am^2/kg, these last used for comparison. They concluded that the MR fluids composed with the EEW nanoparticles showed improved magnetic performance with larger yield stress (~ 1250 Pa for H = 140.1 kA/m) values than the MR fluids with CIP micron sized particles (~ 1150 Pa for H = 140.1 kA/m). This improvement in the measured yield stress value was directly attributed to the lower size and higher saturation magnetization value of the Fe nanoparticles obtained by the EEW technique if compared with the commercial CIP Fe microparticles.

Bearing in mind that magnetic filler parameters like the particle size distribution or its magnetic saturation value are of critical importance in the rheological behaviour of MR fluids, our purpose now is to improve the behaviour of magnetorheological fluids by

using magnetic nanoparticles of FeCo composition with still higher saturation magnetization value than our previously studied pure Fe nanoparticles obtained by the EEW technique. These FeCo nanoparticles will be synthesized through a chemical reduction technique. The obtained product will be extensively analysed and their potential use in MR fluids will be evaluated.

2. Experimental

2.1. Fabrication and characterization of the FeCo nanoparticles.

Iron-cobalt (FeCo) nanoparticles (NPs) were synthesized by employing a chemical reduction technique.[24,25] In this method, aluminium powder was employed as reducing agent to reduce Fe (III) and Co (II). In detail, 5 mmol of iron (III) chloride hexahydrate (1.3515 g.) and 3.75 mmol of cobalt (II) acetate tetrahydrate (0.9341 g.) were dissolved, each one, in 90 ml of ultra-purified water. These solutions were mixed in a three-neck flask. Afterwards, 75 mmol of ammonium fluoride dissolved in 40 ml of ultra-purified water was added to the previous solution in order to stabilize oxidized aluminium as AlF_6^{3-}.This mixture was placed under mechanical stirring during 15 minutes. After that, 10 mmol of aluminium (0.2698 g.) were introduced in the reaction and mixed again by mechanical stirring. The reaction was carried out at 80 ºC in argon atmosphere during 60 minutes. As result, a product in the form of black powder was collected magnetically, it was washed with distilled water and ethanol and dried at room temperature. Thus, the finally obtained powders were subsequently characterized by different techniques. The structure was determined by X-ray diffraction (XRD) measurements by using a PANalytical X'Pert PRO diffractometer equipped with a copper anode (operated at 40 kV and 40 mA), diffracted beam monochromator and Pixel detector. Scans were collected in the 2θ = 10°–90° range, with 0.02° resolution and scan step speed of 1.25 s. The crystallite size was calculated through Scherrer equation.[26]

The morphology of the FeCo nanoparticles, as raw powder and after inclusion in the magnetorheological fluid, was analysed by Transmission Electron Microscopy (TEM) technique. Transmission Electron Microscopy (TEM) micrographs were obtained using a Philips CM200 microscope at an acceleration voltage of 200 kV. For samples preparation both as raw powder and after inclusion in the magnetorheological fluid, FeCo nanoparticles were first dispersed in hexane and drop-casted onto a copper grid. To measure nanoparticles (or their agglomerates) size, ImageJ software was used.

Inductively Coupled Plasma-Mass (ICP) Spectrometry technique was used to determine the final Fe to Co content ratio by using an ICP-MS (7700x, Agilent Technologies) spectrophotometer. To perform this measurement, 30 mg of FeCo nanoparticles were previously dissolved in 2 ml of an acid solution (nitric acid-hydrochloric acid ratio 1:1).

Magnetic properties were measured by using a vibrating sample magnetometer (VSM). Finally, alloy order at the atomic scale was analysed by using Mössbauer spectroscopy. These measurements were performed in transmission geometry using a conventional constant-acceleration spectrometer with ^{57}Co–Rh source. Spectra were collected at room temperature. Isomer shift values were taken with respect to an α-Fe calibration foil. NORMOS program develop by Brand et al. was used for fitting the spectra.[27]

2.2. Synthesis and characterization of the Magneto-rheological Fluids

The FeCo nanoparticles fabricated by the chemical reduction method were used to synthesize different magnetorheological fluids (MRF). For each formulation, mineral oil was used as carrier liquid and Aerosil 300 as additive to control the viscosity of the fluid. More specifically, 46.4 %wt. (0.8172 g.) mineral oil was mixed with 1.2 %wt. (0.0208 g.) of Aerosil 300 in a 5 ml vial. This mixture was dispersed first by ultrasound stirring and afterwards by mechanical stirring, each process lasting for 5 minutes. Then, the surfactant was added and mixed in the same way. As surfactant, we tested first different amounts of oleic acid in order to study its effect in the magneto-rheological behaviour of the fabricated fluids. The best behaviour was found for a fluid containing a 5.3 %wt. (0.0932 g.) content of oleic acid, in the following denoted as FeCo-MR fluid.

A 47.1 %wt. (or 10%vol. content, that is 0.8283 g.) of FeCo NPs was introduced in a two steps procedure: first the 50 % of these NPs is added to the previously prepared mixture and again dispersed first by ultrasound stirring and afterwards by mechanical stirring, each process lasting for 5 minutes. The density of the FeCo nanoparticles was deduced to be 8.3 g/cm^3 from ICP technique results, as it will be further shown. Finally, the remaining 50 % of the FeCo NPs was added to the fluid and first dispersed by ultrasound stirring during 5 minutes and afterwards stirred mechanically during 24 hours at a speed of 150 rpm. This mechanical stirring speed has been the same in all the procedures needed to obtain an appropriate mixture.

In order to get in-situ information about morphology of the FeCo nanoparticles immersed in the fabricated fluid, Small Angle X-Ray Scattering (SAXS) experiments were conducted on a Rigaku 3-pinhole PSAXS-L equipment operating at 45 kV and 0.88 mA. The MicroMax-002+ XRay Generator System is composed by a microfocus sealed tube source module and an integrated X-Ray generator unit which produces CuKα transition photons of wavelength λ=1.54 Å. The flight path and the sample chamber in this equipment are under vacuum. The scattered X-Rays are detected on a two-dimensional multiwire X-Ray Detector (Gabriel design, 2D-200X). This gas-filled proportional type detector offers a 200 mm diameter active area with c.a. 200 micron resolution. The azimuthally averaged scattered intensities were obtained as a function of the wavevector: $q = \frac{4\pi}{\lambda} sin\theta$, being θ half of the scattering angle. Reciprocal space calibration was done using silver behenate as standard. Samples were placed in transmission geometry, with a sample to detector distance of 2 m.

The magneto-rheological behaviour of the obtained magneto-rheological fluids was determined by using an Anton Paar Physica MCR 501 rotational rheometer provided with a MRD70/1T magnetorheological cell and parallel disk configuration (PP20/MRD/TI). The gap employed for the characterization of both fluids has been of 0.58 mm. The magnetic field generated by the MRD70/1T cell is not uniform, but changes from a minimum value at the central zone of the disk to a maximum one nearby the peripheral one. This magnetic field profile is kept for any feeding electrical current intensity, and previous results[28] have already shown that this non-uniformity is enough not to generate any migration of the magnetic fillers within the MR fluid. Thus, the magneto-rheological properties will be measured in a correct way.

The magneto-rheological characterization was performed in three steps: (i) the cell containing the MR fluid spins at 252.4 s^{-1} during 30 s. in order to homogenize it; (ii) the corresponding magnetic field for the measurement is applied during 30 s. and then (iii) the characterization starts keeping the applied magnetic field and starting to increase the shear rate in the range 0.01 to 600 s^{-1}. The shear rate change has been chosen to be logarithmic, so more data have been measured at low shear rate values. To properly measure each shear stress value, measurement last for 3 s. and 60 values of that measured shear stress have been averaged.

3. Results and discussion

3.1. Structural and morphological characterization

Figure 1 shows the obtained XRD pattern of our synthesized FeCo nanoparticles showing the typical peaks ((110) at 45.14º, (200) at 65.67º and (211) at 83º) in agreement with 491568 ICDD files of the α-bcc body-centered FeCo structure, with cell parameter *a*=2.85371 Å.

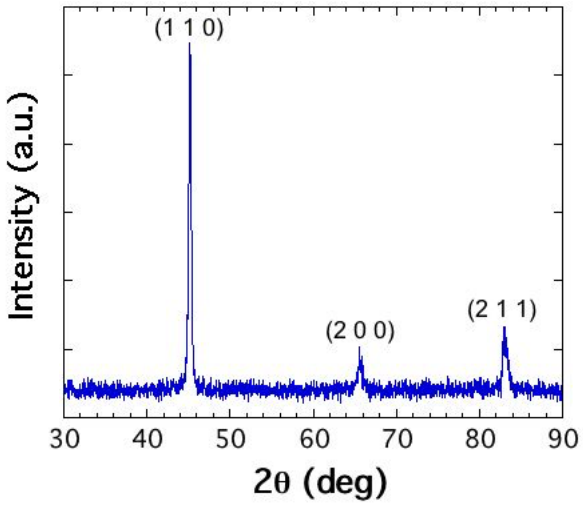

Figure 1. XRD pattern of the raw powder FeCo NPs synthesized by the chemical reduction method.

Oxidized phases or detectable impurities could not be identified in the diffraction pattern. From the full width at half maximum (FWHM) of the (110) diffraction peak, an average crystalline grain size of 42 ± 1 nm was calculated by using the Scherrer's formula. For this estimation, it has to be noticed that the observed peak width stands for values of intensity-weighted size distributions of the different dimensions (as it will be shown in the following) of the nanoparticles.[29]

The morphology of the fabricated raw powder of the FeCo nanoparticles has been studied by analysing TEM images. Figure 2(a) shows that most of the single NPs have a size ranging between 30-50 nm, together with a few plate sized NPs as big as 100 nm. Also and due to the strong magnetic character (high magnetization value) of our FeCo nanoparticles, these TEM images have confirmed the tendency to the aggregate state (see Figure 2(b)) in the form of a dendritic structure as big as 200-500 nm.

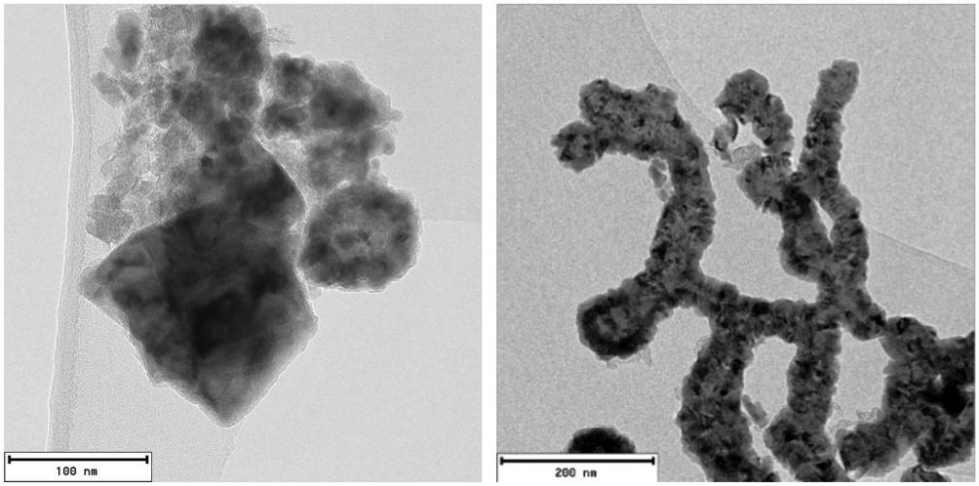

Figure 2. TEM images of the raw powder of FeCo synthesized by the chemical reduction method: (a) single NPs and (b) their agglomeration in a dendritic structure.

We have also analysed the morphology of the synthesized magnetorheological fluid by combining TEM and SAXS techniques. TEM pictures show simultaneously the presence of diluted small nanoparticles as well as big agglomerates of them (see Figure 3(a)). A quantitative analysis of the SAXS results (see Figure 3(b)) is not possible due to the relatively narrow Q-window covered in the experiments and possible contributions from cross-correlations between the FeCo NPs and the other colloidal entities suspended in the fluid. Nevertheless, the SAXS intensity is dominated by the contrast between these ferromagnetic NPs and the rest of the solution and we can qualitatively infer some valuable information from two features observed in the signal: (i) its continuous increase with decreasing Q at the low-Q values region, and (ii) the presence of a minimum at $Q \approx 0.03$ Å^{-1}.

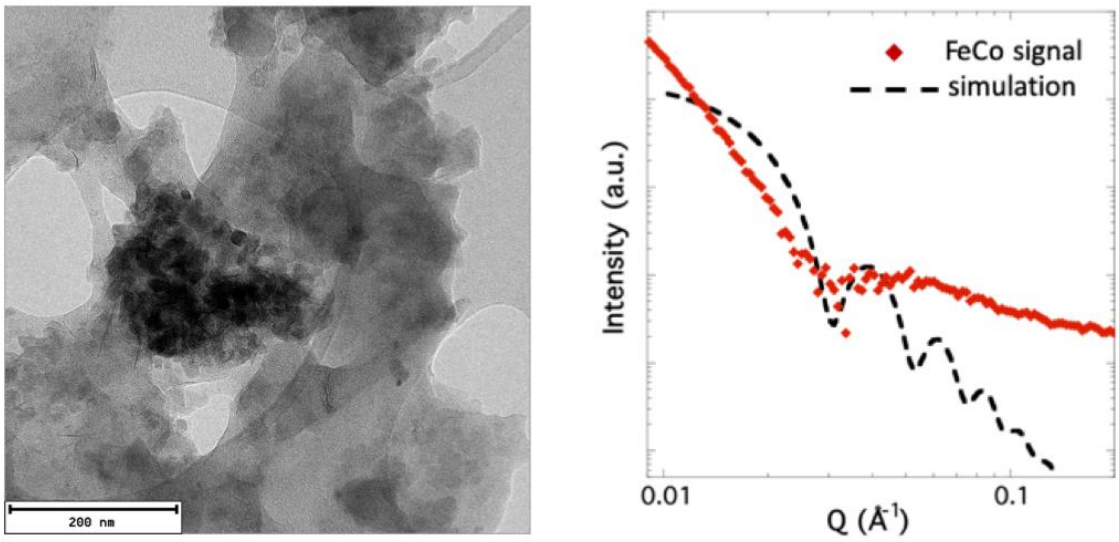

Figure 3. (a) TEM image of the FeCo NPs within the fluid and (b) comparison of the obtained SAXS experimental scattering curve of FeCo-MR (red solid points) with the simulated one (black dashed line).

This minimum is the signature of the form factor of spherical nanoparticles with radius *R*, that occurs at the value of $Q \sim \frac{4.5}{R}$ (see, for example, Equation (5.18) and Figure 5.1 in Roe[30]). Thus, we can deduce a diameter of the spherical entity that translates in our case to the size of the single FeCo fabricated nanoparticle of 30 ± 3 nm from this simple argument.

The comparison of the experimental results with the expected theoretical pattern for a dispersion of individual spherical nanoparticles can be enlightening. This is represented by the dashed line in Figure 3(b). The radii of the spheres considered are narrowly distributed (standard deviation 0.06) around an average value of 14.5 nm. On the one hand, the position of the minimum is rather well reproduced, confirming the previously established size of the particles present within the fluid. On the other hand, the theoretical curve also shows that in the region $Q \to 0$ the expected behaviour for a homogeneous distribution of individual nanospheres is a flattening. However and as previously discussed, our observation is a continuous increase of the scattered signal. This is a clear signature of the presence of agglomerates of the single particles, as previously reported in other mixed systems.[31,32]

From ICP Spectroscopy technique, the final composition of our fabricated NPs turns out to be $Fe_{47}Co_{53}$, slightly deviated from the 1:0.75 ratio of the Fe and Co precursors used for their synthesis or from the $Fe_{50}Co_{50}$ theoretical one.

3.2. Magnetic characterization

Figure 4(a) shows the room temperature hysteresis loop measured for our fabricated $Fe_{47}Co_{53}$ nanoparticles. It shows a rapid saturation with a maximum magnetization value of 212 ± 2 Am^2/kg, remanence magnetization of 18 ± 1 Am^2/kg and low hysteresis with coercivity field value about 7.1 ± 0.1 kA/m (~ 90 Oe).

Before the magnetorheological characterization, we have also measured the room temperature hysteresis loop of the fabricated MR fluid. Figure 4(b) shows a detail of the measured curves for both hysteresis loops (for our raw $Fe_{47}Co_{53}$ nanoparticles, and when immersed in the fluid), at the low applied H field value region and normalized to the M_s = 212 ± 2 Am^2/kg saturation magnetization value. From these curves, two facts merit to be remarked: (i) the slope of the curve corresponding to the FeCo NPs immersed in the fluid is steeper and (ii) the observed coercive field is lower, with a value about 4.6 ± 0.1 kA/m, than the case of the raw FeCo nanoparticles powder. These observations hint clearly for a satisfactory dispersion of the initially aggregated FeCo NPs when the magnetorheological fluid has been fabricated.

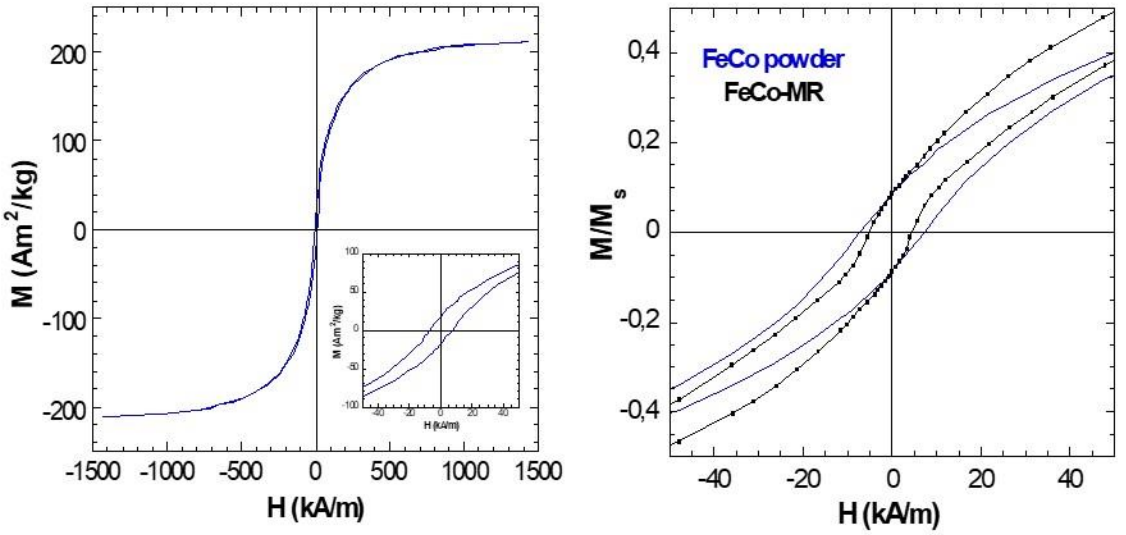

Figure 4. Room temperature hysteresis loop of the raw powder of $Fe_{47}Co_{53}$ NPs synthesized by the chemical reduction method and (b) low applied H field value region measured room temperature hysteresis loops detail for both the raw $Fe_{47}Co_{53}$ nanoparticles powder and the fabricated MR fluid by using those nanoparticles.

The value of the saturation magnetization in the bulk state for pure Fe and Co are well known[33], M_s = 221.9 Am^2/kg and 162.5 Am^2/kg respectively, at room temperature. Also, it is well known the saturation magnetization of the FeCo binary alloy (see Fig. 4.21 in Cullity et al.)[33], that is about 230 Am^2/kg for the equi-atomic $Fe_{50}Co_{50}$ composition. Nevertheless, our measurements give as result a saturation magnetization of 212 ± 2 Am^2/kg, a value that is about an 8% lower than the expected one. This is a usual observation for materials at the nanoscale, as the authors could probe when they studied the CIP (iron carbonyl) nanoparticles.[23] Since magnetic moment of Co atoms does not depend on their environment, but that of Fe does (it increases from 2.2 μ_B in pure Fe to about 3 μ_B in full ordered equiatomic FeCo), our measured saturation magnetization clearly tell us about the atomic level mixing of Fe and Co atoms and subsequent redistribution of spin states in the Fe sites[34], a situation that can be properly described by using Mössbauer spectroscopy technique.

Figure 5(a) shows the ^{57}Fe Mössbauer spectrum corresponding to the FeCo synthesized powder sample. The spectrum presents an only well resolved sextet with an average hyperfine field of around B_{hf} ~ 35 T. The characteristic 33 T signal of the bcc-Fe is absent which indicates that all the Fe atoms are in the FeCo alloy and no clusters of bcc-Fe are shown up. The spectrum is almost symmetrical, denoting high symmetrical crystallographic locations for the Fe atoms and confirming therefore a cubic structure of the alloy.

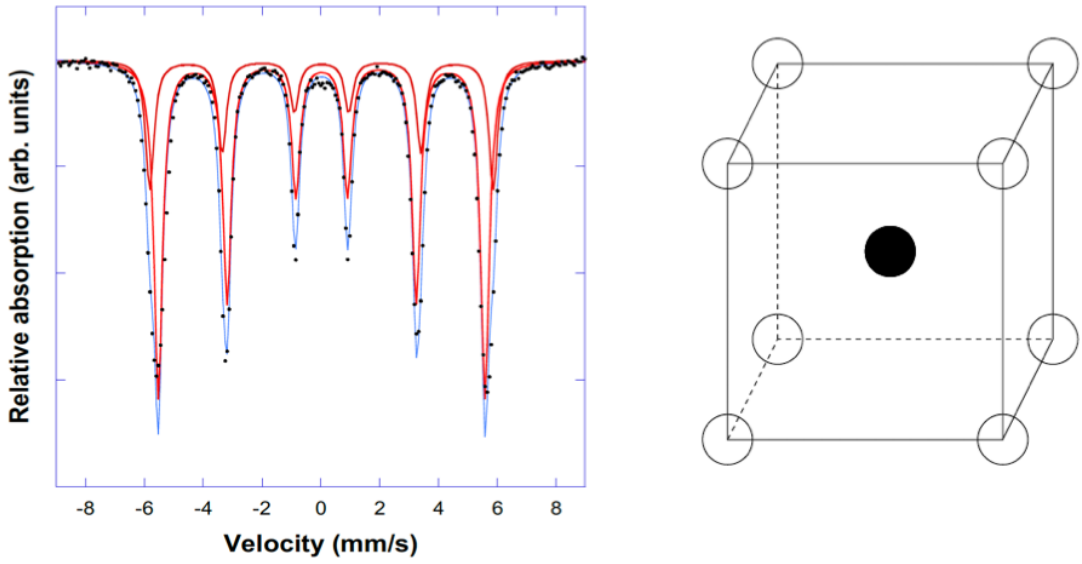

Figure 5. (a) Room temperature Mössbauer spectrum and (b) ordered B2 structure of the FeCo NPs synthesized by the chemical reduction method.

In an equiatomic FeCo alloy with a B2 cubic structure (see Figure 5(b)), Co and Fe atoms are located in a D and A positions respectively. Out of $Fe_{50}Co_{50}$ stoichiometry, excess of Co atoms randomly substitutes Fe atoms exclusively in A position. As these different chemical environments around the Fe atoms are situated in their second next neighbourhood, the influence of these non-equivalent chemical settings on the hyperfine parameters of the spectra of Fe atoms is reduced. According to the ICP analysis, the actual composition of the synthesized NPs is $Fe_{47}Co_{53}$, fixing the relative number of Fe atoms in A position down to 94%. Considering a binomial distribution of Fe and Co atoms, the relative probability of locating a Co atom as a second next neighbour for a Fe atom would be of 27%. The presence of a Co atom would induce a slightly higher hyperfine field in the nucleus of the Fe. We have fitted the experimental spectrum by means of two contributions, considering or not respectively the presence of a Co atom in the second next neighbourhood of the Fe atoms. The relative areas have been fixed according to the relative abundance of these two probable chemical environments. As it can be observed in Figure 5a the measured experimental spectrum is properly modelled, a fact that would validate the $Fe_{47}Co_{53}$ stoichiometry as obtained from ICP analysis. Both contributions present similar isomer shifts values of δ~0.03 mm/s, zero quadrupolar shifts and widths close to 0.3 mm/s.

3.3. Magnetorheological characterization

In magnetorheological fluids, the formation of magnetic field induced structures is only expected when the λ ratio is large enough. In Table I, the calculated values of λ following equation (2) (assuming $\mu_{cr} \approx 1$, $\beta \approx 1$ and $s << a$) and using the magnetic strengths that will be further applied in the magnetorheological characterization, are shown. This equation (2) is only valid for magnetically soft multidomain particles, as it happens with our FeCo nanoparticles (see an extensive explanation in Suplementary Material S1). According to the obtained values, we can affirm that are the aggregates (as big as 500 nm) of small nanoparticles of the FeCo alloy, which mainly contribute to the formation of those field-induced structures, at any applied magnetic field. On the contrary, the smallest nanoparticles (30 nm) at the smallest applied magnetic field-intensities, behave as being constituents of a ferrofluid. As a whole and due to the simultaneous presence of small nanoparticles (30-50 nm size) and their aggregates (200-500 nm), our fabricated fluid behaves as a magnetorheological fluid.

Table I. λ ratio for our fabricated MRF containing FeCo nanoparticles or their aggregates, calculated under the action of the applied magnetic strengths used in the magnetorheological characterization. Shaded values correspond to $\lambda \leq 1$ values, while white region corresponds to $\lambda > 1$ ones.

H_0 (kA/m)	Diameter (nm) = 2*a*			
	30	50	200	500
12.7	0.26	1.2	76.9	1200
26.1	1.095	5.07	324.5	5070
67.9	7.41	34.3	324.5	3.43×10^4
140.1	31.5	145.9	9339.4	1.46×10^5
280.9	126.9	587.4	3.76×10^4	5.87×10^5
616.7	611.1	2829.2	1.81×10^5	2.83×10^6

Further, we have measured the rheological properties (the flow and deformation under applied force) of our synthesized MR fluids from bulk samples and by using a mechanical rheometer. Under application of an external magnetic field, we have observed that our fabricated MR fluids showed a non-Newtonian behaviour.[35] Thus, a correct analysis of the data has been performed by applying the Rabinowitsch conversion method.[36-38]

The externally applied magnetic field has been ranged from 0 to 616.7 kA/m, and after each characterization measurement, a demagnetization cycling procedure was applied. Both the studied fluids with a 10%vol. concentration of nanoparticles showed a strong magnetorheological response as demonstrated by the increase measured shear stress values as the magnetic field intensity increases (see Figure 6). Nevertheless, for the two upper curves of the Fe-EEW fluid a slight decrease of the shear stress when the shear rate increases can be noticed. The authors have previously observed these jumps in other commercial samples, which have been ascribed to wall slip behaviour between the plate and the sample (see Figure S2.1 (a) in Supplementary Material S2).

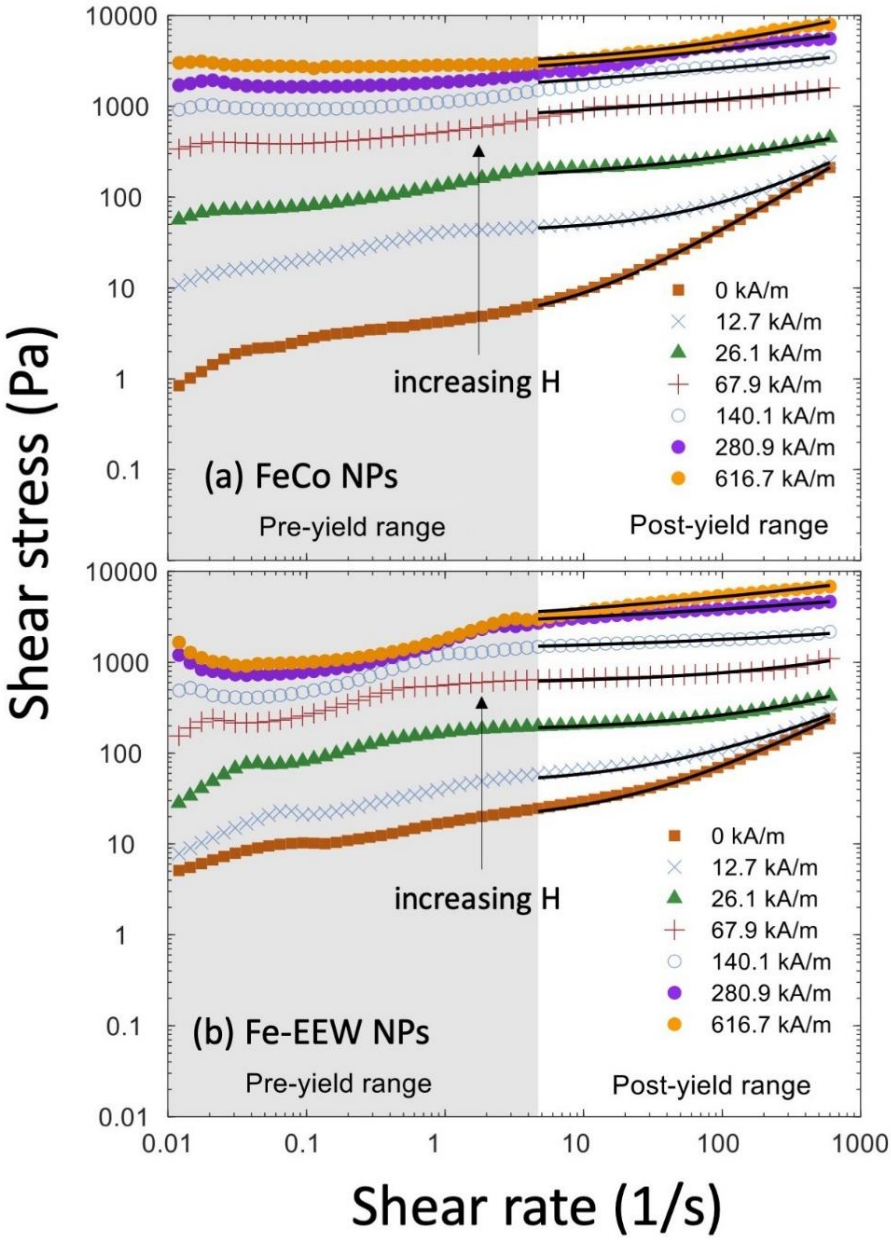

Figure 6: Rheological curves as a function of the applied magnetic field: (a) for the new FeCo-MR fluid studied and (b) the one fabricated with Fe nanoparticles obtained by the EEW technique. Black lines show the Herschel-Bulkley fit for several applied magnetic field cases. In both fluids, a 10%vol. concentration of nanoparticles was employed.

The measured rheological curves of both fluids under application of an external magnetic field were characterized by the corresponding yield stress value. Again and in both tested MR fluids the magnitude of this yield stress increases as the magnetic field intensity does. Moreover, in both cases, the post-yield behaviour can be described as a pseudo-plastic one.

Obtained data from rheological measurements were fitted by using the Herschel-Bulkley model[39] that accounts for the parametric description of the rheological post-yield behaviour of both magnetic fluids as a function of the magnetic field intensity:

$$\tau = \tau_0 + K \cdot \dot{\gamma}^n \quad (4)$$

where τ is the shear stress, τ_0 is the yield stress, $\dot{\gamma}$ is the shear rate, K is the consistency index (that gives an idea about the viscosity of the fluid) and n is the pseudo-plasticity or flow behaviour index (for pseudo-plastic fluids, $n<1$).[39] In order to take into account shear thinning, the Herschel-Bulkley model, in which the post-yield plastic viscosity is dependent on shear strain rate has been used.[2] In fact, in Figure 6 the obtained fitting curves for all applied magnetic fields are also shown. The regression coefficients (R^2) of the fittings for shear rates $\dot{\gamma} \geq 5$ s^{-1} are all above 0.91. For the MR fluid containing the FeCo nanoparticles, it has to be noticed that at the maximum applied magnetic field of 616.7 kA/m, there is an almost full coincidence between measured experimental points and obtained fitting curve. At lower shear rates and measured shear stresses, instead, the fit with a Herschel-Bulkley model is not appropriate, as it doesn't take into account neither the visco-elastic effects nor interactions among nanoparticles appearing in the pre-threshold region.[40] Previous work from several authors[41,42] have already tested several phenomenological models for such pre-threshold region, arriving to the conclusion that classical models like the Maxwell model, Kelvin-Voigt model, or the combination of both[39] should be used. However, such a study is outside the aim of the present work.

Figure 7 shows the dependence of the obtained parameters obtained from the fit with equation (4) versus the applied magnetic field intensity, for both the studied MR fluids. As expected, the dynamic yield stress values τ_0 for the fluids containing Fe and FeCo nanoparticles are quite similar and increase as the applied magnetic field does. However and for the Fe nanoparticles containing fluid, this yield stress remains almost constant at a value of $\tau_0 \approx 2\ kPa$ beyond the applied field of 140.1 kA/m.

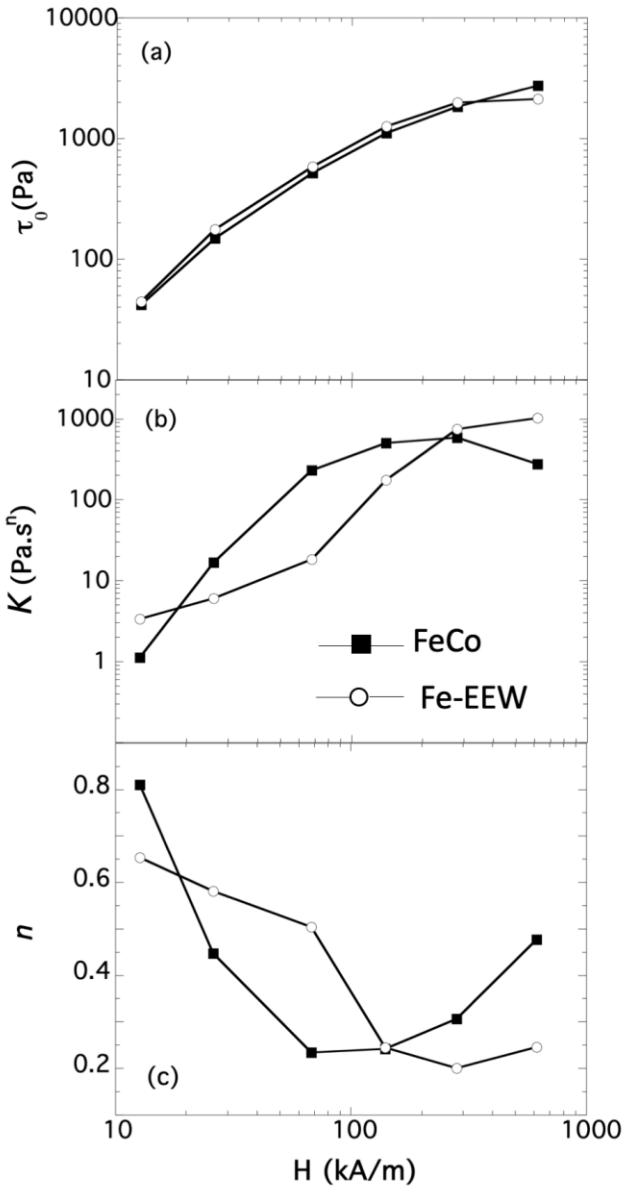

Figure 7. Obtained Herschel-Bulkley model parameters for different applied magnetic fields and for both the studied FeCo and Fe nanoparticles containing fluids: (a) yield stress τ_0, (b) consistency *K*, and (c) pseudo-plasticity index, *n*.

The reason for this observation arises most probably from the effect of these nanoparticles agglomeration in the fluid magnetorheological behaviour, as it will be further discussed. This yield stress behaviour is accompanied by a progressive increase of the viscosity of the fluid, as the increase of consistency index *K* indicates, while the flow behaviour index *n* keeps, in all cases in the range $0.2 < n < 0.8$ assuring so the pseudo-plastic character of our studied magnetorheological fluids.

According to the $\lambda > 1$ values criterion, only large particles under large applied magnetic fields should form field-induced structures within the fluid. These field-induced structures change the viscosity of the MRF, and so a large magnetization of the magnetic fillers will lead to a larger field-induced viscosity. During the measurement the hydrodynamic forces lean to break the field-induced structures, while the magnetic and the surface forces lean to keep them undamaged.[43] There are two possible mechanisms expected to govern this force balance, conducting both to these structures destruction. On the one hand, "bulk destruction mechanism" occurs when the tensile hydrodynamic and tensile magnetic forces overcome the compressive surface tension force, what leads to mechanically unstable structures. In that case, the structure is expected to break in smaller parts and the structure rupture can be seen as a bulk destruction process. On the other hand, "erosion destruction mechanism" happens when the magnetic particles worn away from the structure surface due to the hydrodynamic forces. When these erosive forces overcome the adhesive magnetic ones, the structure size decreases until the equilibrium is re-established. Zubarev et al.[43] studied both above described mechanisms separately for a better understanding of the influence of each one, despite these mechanisms may act simultaneously.

Both mechanisms give qualitatively different rheological behaviours considering the dimensionless Mason numbers as it will be further discussed. Zubarev's definition of Mason number, defined through magnetic field strength *Mn(H)*, is equivalent to the Klingenberg's[44] definition of mason number through suspension magnetization or particle magnetization *Mn(M)*, according to the linear magnetization law. However, at high field strength the suspension magnetization exhibits a non-linear behaviour, so *Mn(M)* allows a better representation of experimental results in the broad range of the magnetic fields.

$$Mn(M) = \frac{9}{2}\frac{\eta_c \dot{\gamma} \phi^2}{\mu_0 \mu_c \langle M \rangle^2} \tag{5}$$

where η_c and μ_c are the base fluid (mineral oil + Aerosil 300 + oleic acid) viscosity and permeability, respectively; ϕ is the FeCo nanoparticles volumen fraction (10%vol. or ϕ =0.1), and $\langle M \rangle$ is the suspension magnetization (see MR fluid hysteresis loop in Supplementary Material S1). On the other hand, the dimensionless viscosity is defined as the measured apparent viscosity of the suspension (η_{app}) divided by η_∞, where this η_∞ is considered as the viscosity of the suspension at high shear rate in absence of magnetic

field.[44] Figure 8 shows the scaling of the measured dimensionless viscosity curves with this Mason number *Mn*.

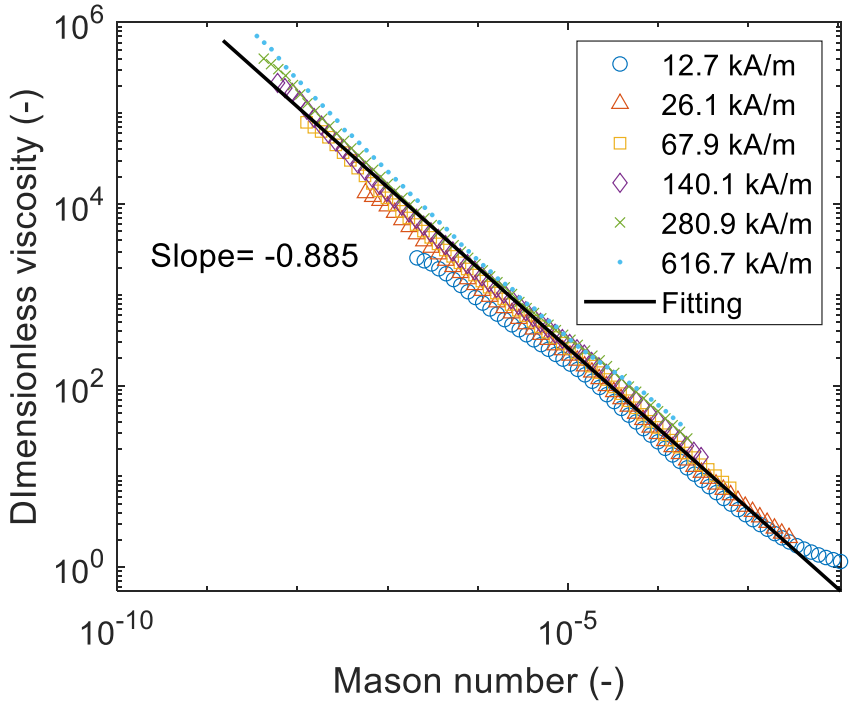

Figure 8. Measured dimensionless viscosity as a function of Mason number, *Mn*. Data correspond to all employed $\dot{\gamma}$ rates.

The ability of *Mn* as defined by equation (5) to collapse our experimental data is clearly observed. This collapse is rather good and happens with $\lambda > 1$, for all applied magnetic field strengths and independently of the FeCo nanoparticle size, single or agglomerated. According to Zubarev et al.[43] studies, the bulk destruction mechanism presents a power-law $[\eta] \propto M_n^{-2/3}$ behaviour and the erosive destruction scenario provides another scaling for the field-specific viscosity $[\eta] \propto M_n^{-4/5}$. As is shown in Figure 8, the experimental data follow a simple power-low trend and gather into a single master curve with an exponent of 0.885. So, even if both destruction mechanisms are taking part in the measurement, the fluid shows a preference to an erosive destruction mechanism.

Similar results have been previously observed by other authors in the case of dilute conventional MR fluids[45] or particles in the borderline between FF and MRF fluids[16]. From those observed collapses, it has been inferred that is the particle magnetization that governs the rheological behaviour. This is what occurs especially in the case, since we have used FeCo nanoparticles (or their agglomerates) with their high magnetization value in the fabrication of the new MRF.

In which concerns the measured dynamic yield stress value as a function of applied magnetic field strength H_0, the analysis of the observed slope change can provide an interesting insight. Fang et al.[46] examined dynamic yield stress (τ_0) dependence on the applied magnetic field strength H_0 and divided the observed behaviour in different regimes: briefly, the low H_0 field region, in which $\tau_0 \propto H_0^2$ due to the local saturation of magnetic fillers; intermediate H_0 zone, in which $\tau_0 \propto H_0^{3/2}$; finally, when the applied field strength high enough to achieve the magnetic saturation of the fluid and τ_0 is almost independent of applied magnetic field and scales as the saturation magnetization of the fluid. They also proposed the existence of a critical magnetic field value H_C that separates the low field from the moderate applied magnetic field strength regime. These differentiated regimes have been confirmed in magnetorheological fluids fabricated with high magnetization CI (carbonyl iron) microparticles: CI (4 μm in size)+SWCNT (single-walled carbon nanotubes,[46] and CI (4 μm in size)+polyaniline+MWCNT (multiwall carbon nanotubes)[47], and more recently in MR fluids with moderate magnetization filler (hollow nanometric magnetite).[48]

Figure 9 shows our results for similar fits derived for our MR fluids fabricated with FeCo (size ranging from 30-50 nm to 500 nm, aggregates) and Fe-EEW nanoparticles (about 77 nm, possible aggregates). In both cases two different behaviours against the applied magnetic field strength H_0, can be distinguished, as well as the critical field that divides those regions. For the FeCo nanoparticles containing MR fluid, we found an initial region with $\propto H_0^{1.49}$ dependence, a critical filed H_C = 95.1 kA/m, and a second region showing $\propto H_0^{0.61}$. When Fe-EEW nanoparticles have been used to fabricate the MR fluid, we found an initial region with $\propto H_0^{1.52}$ dependence, a critical filed H_C = 104.9 kA/m, and a second region showing $\propto H_0^{0.35}$. If compared with results obtained when using CI microparticles[46,47] the obtained values from our measurements fits merit several comments: first, the obtained critical field value is close in all cases, about 100 kA/m. However, this fitted critical field value will not divide strictly the applied low and the intermediate magnetic field zones.

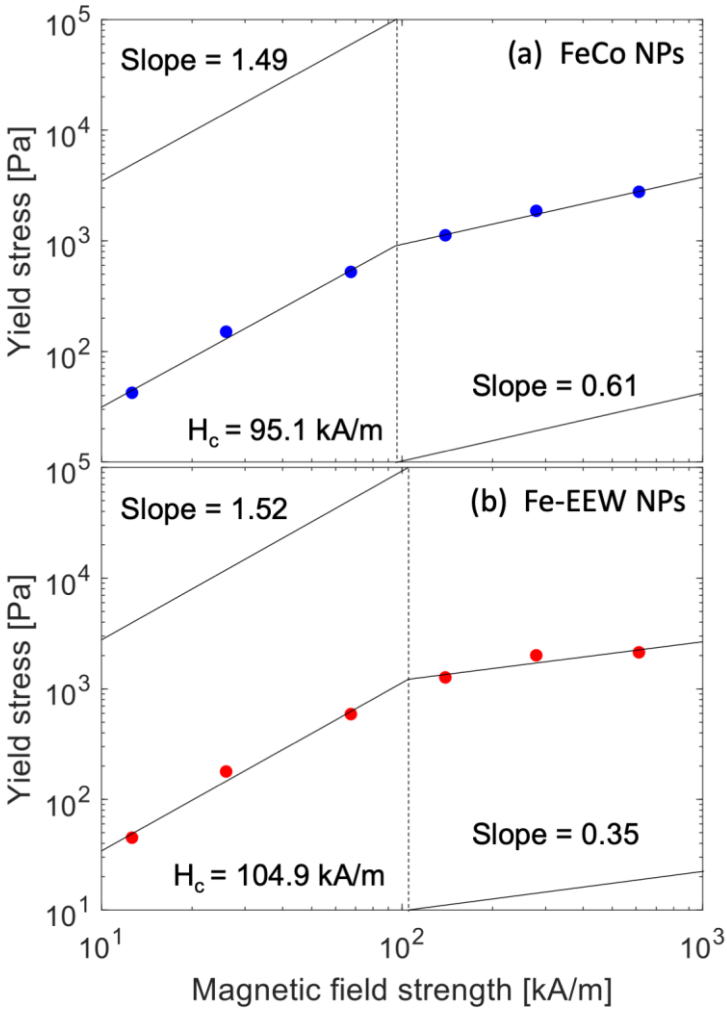

Figure 9. Dynamic yield stress behaviour plotted as a function of magnetic field strength for (a) the new FeCo-MR fluid studied and (b) the one fabricated with the Fe nanoparticles obtained by the EEW technique.

The first region we can determine has a slope very close to 3/2 = 1.5, that is we observe directly the intermediate H_0 zone, and there is no trace of the low applied magnetic strength zone. This fact can be understood if we bear in mind that prior to each magnetorheological measurement a demagnetization cycling procedure was applied, and any magnetic remanence has been minimized practically to zero. So, if in absence of applied magnetic field there is still some particle aggregation within the MR fluid, this has to arise from an inadequate surfactant recovering of the magnetic nanoparticles, remaining some particle aggregation due to the dipolar interaction among them, but not strictly speaking from the remanence itself. The application of external magnetic field for the MR measurements leads the nanoparticles to their agglomeration (as previously shown for the FeCo nanoparticles in section 3.1 of this work) within the MR fluid. Thus,

within the fabricated fluid we have not only the strong magnetic dipole-dipole interaction among single small FeCo nanoparticles, but also single NP-agglomerate and agglomerate-agglomerate strong magnetic interaction contributions. Thus, the effect of the applied magnetic field is quickly enhanced and drives the fluid easily to magnetic saturation. In fact, applied magnetic fields of 12.7 and 67.9 kA/m (limits of this first region) makes the fluid to achieve already a 22% and 58% respectively of the fluid saturation magnetization. Beyond the critical filed H_C, the increasing slope exhibited by the yield stress falls drastically to a value of 0.61, hinting for the fully magnetic saturation of the fluid and consequent pinning of the formed magnetic fillers chains. At an applied magnetic field of 616.7 kA/m (the maximum allowed for our magnetorheological characterization equipment), the FeCo MR fluid has reached already the 96% of its measured magnetic saturation (see MR fluid hysteresis loop in Supplementary Material S1).

Similar behaviour has been found for the Fe-EEW containing MR fluid, and so we can infer also that some degree of agglomeration is also present within this fluid. It is worthy to mention that the slope determined for the second region is of 0.35, lower than that of the FeCo MRF. This is in direct correlation with the approach to magnetic saturation observed for both type of nanofillers, faster in the case of the Fe-EEW nanoparticles than for the FeCo ones (see hysteresis loops in Supplementary Material S1).

But whenever the case, the application of external magnetic field for the MR measurements, drives quickly the nanoparticles to agglomeration, giving rise to non-reversible behaviour, stronger for the Fe-EEW NPs that for the FeCo ones, as it is further shown in Figure 10: here the measured rheological curves after applying a magnetic field to each studied MR fluid and a subsequent demagnetization process are presented. For the shake of clarity, only shear rates up to 100 s^{-1} are shown. At a first glance it is clear that the MR fluid containing FeCo high magnetization NPs exhibits a much more reversible behaviour that the Fe NPs containing fluid. Even with the highest applied magnetic field values, after demagnetization the FeCo-MR fluid goes back to its initial state keeping almost constant its yield stress value. This reversibility is only observed for the Fe-MR fluid for applied magnetic fields up to 140.1 kA/m.

To give a number to this irreversibility, we have estimated a dispersion of the measured shear stress, in both cases at the shear rate of 10 s^{-1}, of about a 18% for the FeCo-MR fluid and about a 39.5% for the Fe-MR fluid one.

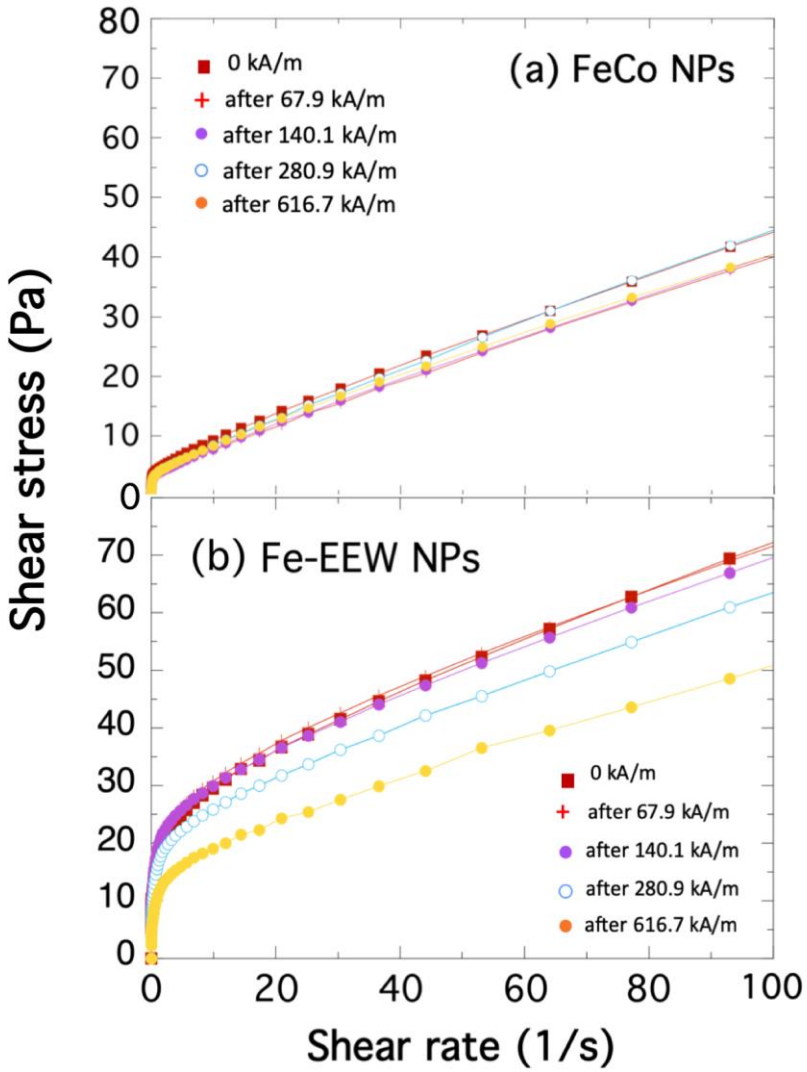

Figure 10. Rheological curves after applying magnetic field and demagnetizing process for both the studied FeCo and Fe nanoparticles containing fluids.

Aiming to compare our results with previous ones, we have done an extensive bibliographic research looking for works where strictly FeCo nanoparticles were used to fabricate MR fluids. We have found only two publications that describe a MR fluid properties uniquely composed of FeCo nanoparticles as magnetic filler: the first one by Lambrick et al.[49], where the authors describe the fabrication process of different fluids containing extremely fine nanoparticles (5 - 8 nm), but no information about neither the quality of the synthesized FeCo alloy nor magnetorheological behaviour of the fabricated different fluids is given.

The second work was performed by Injamamul Arief et al.[50] and the authors report the synthesis of $Fe_{55}Co_{45}$ (close to our alloy composition) acetate-polymer capped and citrate-capped particles and the magnetorheological behaviour of two different fluids fabricated by using those particles as magnetic fillers. Therein the reader can find an extensive description of particles preparation, structure, morphology, magnetic properties and magnetorheological properties of the subsequent fabricated fluids. Summarizing the results presented in this work, the best results achieved correspond to the citrate-capped particles of about 0,7 microns size, saturation magnetization below 200 Am^2/kg , and yield stress value (following the Herschel-Bulkley model behaviour) of about 600 Pa for an applied magnetic field of 1,2 T = 955,2 kA/m.

In front of these results, our work has truly improved all the previously mentioned properties: we have fabricated very good quality $Fe_{47}Co_{53}$ alloy nanoparticles with high saturation magnetization value (212 Am^2/kg) and good magnetorheological response with yield stress value (following again the Herschel-Bulkley model behaviour) of about 2729 Pa for an applied magnetic field of 616,7 kA/m.

Therefore and to sum up with all our previous observations, we can affirm that we have fabricated a magnetorheological fluid (as derived from calculated λ ratio values and observed collapse of experimental data plotted against Mason number, *Mn*) with high magnetization nanoparticles as magnetic fillers. These nanofillers are single nanoparticles (ranging from 30 to 50 nm) or their agglomerates (ranging from 200 to 500 nm), but always at the nanosize. The strong magnetic dipole-dipole interaction among nanofillers drives the fluid quickly to magnetic saturation improving both the values obtained for yield stress and the observed reversibility after demagnetization process, if compared with the previously obtained also by the authors when using Fe-EEW high magnetization nanoparticles as magnetic fillers of the fluid. Future work points towards a modified fabrication process of the FeCo nanoparticles in order to prevent them from agglomeration, followed by the correspondent nanoparticles sedimentation behaviour within the fluid study.

Finally, Table II contains a comparative analysis of some magnetorheological fluids containing Fe, Fe_3O_4 and Fe-Co micro- and nanoparticles as magnetic fillers, as reported in recent literature.

Table II. Comparison of different MR fluids prepared with high magnetization micro and nanoparticles of Fe, Fe_3O_4 and Fe-Co as magnetic fillers.

Reference	Particle composition	Particle size (nm)	Particle concentration (vol.%)	Carrier	Magnetic field (kA/m)	Yield stress (Pa)
[23]	Fe (CIP)	1100	10	Mineral oil	140.1	1150
[23]	Fe (EEW)	77	10	Mineral oil	140.1	1250
This work	Fe (EEW)	77	10	Mineral oil	616.7	2106
This work	FeCo	30-50	10	Mineral oil	140.1	1105
This work	FeCo	30-50	10	Mineral oil	616.7	2729
[5]	Fe (arc plasma)	104	15	Silicone oil	79	1500
[5]	Fe (arc plasma)	104	15	Silicone oil	159	3100
[5]	Fe (arc plasma)	104	15	Silicone oil	238	5500
[51]	Fe	4	20	Lubricant oil	343	20
[52]	Fe_3O_4@mSiO_2	260	5	Silicone oil	171	38
[53]	Fe (DC arc)	30-50	40	Silicone oil	434	4200
[54]	$CoFe_2O_4$(*)	38	8.24	Silicone oil	250	4800

(*) Co ferrite nanoparticles not immersed in a fluid, but deposited into a MoS_2 nanosheet

From the values appearing in the table we can infer two interesting observations: first, that to use a high magnetization nanofillers is not a guarantee of fabricating a good magnetorheological fluid, as Kim et al. show in their work.[51] Second, that the authors of this work report measurements with the highest applied magnetic field, up to 616.7 kA/m. Besides and using only a 10%vol. concentration of FeCo nanoparticles, we have measured yield stress values that compete well with the highest reported ones.[5,54]

4. Conclusions

FeCo high magnetization (212 ± 2 Am^2/kg) magnetic nanoparticles have been fabricated by using the chemical reduction technique. XRD analysis confirmed the good cristallinity of the pure FeCo alloy and TEM and SAXS gave as results nanoparticles of size ranging among 30-50 nm that easily agglomerate in bigger entities of about 200-500 nm due to the strong magnetic dipolar interaction between the nanoparticles.

These FeCo nanofillers were used to synthesize a magnetorheological fluid (FeCo-MR) by using oleic acid as surfactant, mineral oil as carrier liquid and Aerosil 300 as additive to control the viscosity of the fluid. For comparison, we have also tested a previously reported Fe (Fe-EEW) nanoparticle containing MRF fluid by applying magnetic fields up to 616.7 kA/m. Both these studied fluids showed a strong magnetorheological response with increasing shear stress values as the magnetic field intensity increases, behaviour that was fitted by using the Herschel-Bulkley model.

The Fe-EEW MRF shows a good magnetorheological response for applied magnetic fields up to 140.1 kA/m, with a yield stress value of 1250 Pa. For higher values of the applied magnetic field, there are evidences of Fe nanoparticles agglomerates that perturb the magnetorheological response of this fluid. However, our new FeCo-MR fluid shows superior performance up to 616.7 kA/m, with a yield stress value of 2729 Pa. This value competes with the best ones reported in the most recent literature. We also have observed a good reversibility after demagnetization process of the our new FeCo-MR fluid, much better than the one measured for the Fe-EEW magnetorheological fluid.

Future work points towards the fabrication of a magnetorheological fluid containing magnetic nanoparticles of $Fe_{70}Co_{30}$ with a well defined size distribution and saturation magnetization of 240 Am^2/kg, fabricated by following a modified chemical route in order to prevent them from agglomeration. This should be followed by the correspondent nanoparticles sedimentation behaviour within the fluid study.

Acknowledgements

J. Berasategi, A. Gómez and M.M. Bou-Ali would like to thank the financial support provided by the Basque Government under research project PI-2017-1-0055 and MMMfavIN (KK-2020/00099, Elkartek program). V. Vadillo, J. Gutiérrez, J.M. Barandiarán, M. Insausti and I. Gil de Muro would like to thank the financial support provided also by the Basque Government under PI-2017-1-0043, the MMMfavIN (KK-2020/00099, Elkartek program) and Research Groups (IT1245-19 and IT1226-19) research projects. A. A. and A.I. gratefully acknowledge the financial support of the Basque Government (Research Groups IT-1175-19) and the Ministerio de Economía y Competitividad (PGC2018-094548-B-I00, MCIU/AEI/FEDER, UE). Technical and human support provided by the General Research Services of the UPV/EHU (SGIker) is gratefully acknowledged. In particular, extensive and deep discussions with Dr Iñaki Orue about magnetic behaviour of nanoparticles is truly appreciated.

References

1. JD Carlson, MR Jolly, MR fluid, foam and elastomer devices, Mechatronics, 2000 **10**, 555-569.
2. F Goncalves A Review of the State of the Art in Magnetorheological Fluid Technologies - Part I: MR fluid and MR fluid models, Shock Vib. Dig., 2006, **38,** 203–219.
3. J De Vicente, D J Klingenberg, R Hidalgo-Alvarez, Magnetorheological fluids: a review, Soft Matter, 2011, **7**, 3701-3710.
4. SW Charles, The preparation of magnetic fluids in Ferrofluids, Stefan Odenbach (Ed.): LNP, 2002 **594**, 3–18.
5. J Noma, H Abe, T Kikuchi, J Furusho, M Naito, Magnetorheology of colloidal dispersion containing Fe nanoparticles synthesized bythearc-plasma method, J. Magn. Magn. Mater., 2010, **322**, 1868–1871.
6. C Kormann, H M Laun, H J Richter, MR fluids with nano-sized magnetic particles, Int. J. Mod. Phys. B, 1996, **10**, 3167 – 3172.
7. J M Ginder, L C Davis, Shear stresses in magnetorheological fluids: Role of magnetic saturation. Appl. Phys. Lett., 1994, **65**, 3410-3412.
8. MR Jolly, JD Carlson, BC Muñoz, A model of the behaviour of magnetorheological materials. Smart Mater. Struct., 1997, **5,** 607-612.
9. J M Ginder, Behaviour of magnetorheological fluids, MRS Bull, 1998, **23**, 26-29.
10. G Bossis, O Volkova, S Lacis, A Meunier, Magnetorheology: Fluids, Structures and Rheology in Ferrofluids. Edited by S. Odenbach (Springer, Bremen, Germany) 2002, 202.
11. R.E Rosensweig, Ferrohydrodynamics, Dover, New York, 1997.
12. R E Rosensweig An introduction to ferrohydrodynamics Chem. Eng. Commun. 1988, **67,** 1.
13. S Odenbach, Ferrofluids—magnetically controlled suspensions, Colloid Surf. A 2003, **217**, 171.
14. I V Beketov, A P Safronov, A I Medvedev, J Alonso, G V Kurlyandskaya, S M Bhagat, Iron oxide nanoparticles fabricated by electric explosion of wire: Focus on magnetic nanofluids, AIP Adv., 2012, **2**, 022154.
15. J Nowak, D Wolf, S Odenbach, A rheological and microscopical characterization of biocompatible ferrofluids, J. Magn. Magn. Mat., 2014, **354**, 98 – 104.

16. K Sharivar, J R Morillas, Y Luengo, H Gavilan, P Morales, C Bierwisch Rheological behaviour of magnetic colloids in the borderline between ferrofluids and magnetorheological fluids, J. of Rheology, 2019, **63,** 547 – 558.
17. S Odenbach, K Raj, The influence of large particles and agglomerates on the magnetoviscous effect in ferrofluids, Magnetohydrodynamics, 2000, **36,** 312 – 319.
18. MT López-López, J de Vicente, G Bossis, F González-Caballero, JDG Durán Preparation of stable magnetorheological fluids based on extremely bimodal iron–magnetite suspensions, J. Mater. Res., 2005, **20,** 874-881.
19. J De Vicente, M T López-López, F González-Caballero, JDG Durán, Rheological study of the stabilization of magnetizable colloidal suspensions by addition of silica nanoparticles, J. Rheol, 2003, **47**, 1093-1109.
20. RC Bell, JO Karli, AN Vavreck, DT Zimmerman, GT Ngatu, NM Wereley, Magnetorheology of submicron diameter iron microwires dispersed in silicone oil. Smart Mater. Struct., 2008, **17**, 015028.
21. P Kuzhir, M T López-López, G Bossis, Magnetorheology of fiber suspensions. II Theory, Journal of Rheology, 2009, **53**, 127-151.
22. AJ Margida, KD Weiss, JD Carlson, Magnetorheological materials based on Iron alloy particles, Int. J. of Modern Physics B, 1996, **10**, 3335 – 3341.
23. J Berasategi, A Gomez, MM Bou-Ali, J Gutiérrez, JM Barandiarán, IV Beketov, AP Safronov, GV Kurlyandskaya Fe nanoparticles produced by electric explosion of wire for new generation of magneto-rheological fluids. Smart Mater. Struct., 2018, **27**, 045011(8 pp.); doi: 10.1088/1361-665X/aaaded.
24. B Kandapallil, RE Colborn, PJ Bonitatibus, F Johnson, Synthesis of high magnetization Fe and FeCo nanoparticles by high temperature chemical reduction. J. Magn. Magn. Mater, 2015, **378**, 535–538.
25. Z Klencsár, P Németh, Z Sándor, T Horváth, IE Sajo, S Mészáros, J Mantilla, JAH Coaquira, VK Garg, E Kuzmann, Gy Tolnai, Structure and magnetism of Fe-Co alloy nanoparticles. J. Alloys Compd., 2016, **674**, 153–16.
26. R Jenkins, RL Snyder, Introduction to X-ray Powder Diffractometry, John Wiley & Sons Inc., 1996, 89-91.
27. RA Brand, Normos Mössbauer Fitting Program, Univ. Duisburg, 2002.
28. HM Laun, G Schmidt, C Gabriel, C Kieburg, Reliable plate–plate MRF magnetorheometry based on validated radial magnetic flux density profile simulations, Rheologica Acta, 2008, **47**, 1049-1059.

29. A Valério, SL Morelhao, Usage of Scherrer's formula in X-ray diffraction analysis of size distribution in systems of monocrystalline nanoparticles, 2019, arXiv:1911.00701v1 [cond-mat.mtrl-sci].
30. RJ Roe, Methods of X-Ray and Neutron Scattering in Polymer Science, Oxford University Press, New York, 2000.
31. P Deb, A Basumallick, D Sen, S Mazumder, BK Nath, D Das, Anomalous agglomeration characteristics observed in iron oxide nanoclusters. Philosophical Magazine Letters, 2006, **8**, 491–499.
32. F Döbrich, A Michels, R Birringer, Synthesis of a nanorod ferrofluid and characterisation by magnetic-field-dependent small-angle X-ray scattering, J. Magn. Magn. Mater., 2007, **316**, e779–e782.
33. BD Cullity, CD Graham, Introduction to Magnetic Materials. 2nd edition, IEEE Press & John Wiley & Sons Inc. Publication, 2009, ISBN: 978-0-471-47741-9, Table 4.2, p. 127.
34. T Sourmail, Near equiatomic FeCo alloys: constitution, mechanical and magnetic properties. Progress in Mater. Sci., 2005, **50**, 816-880; and references therein.
35. O Ashour, CA Rogers, W Kordonsky, Magnetorheological Fluids: Materials, Characterization, and Devices, J. Intell. Mater. Syst. Struct., 1996, **7**, 123-130.
36. M Zubieta, MJ Elejabarrieta, MM Bou-Ali, A numerical method for determining the shear stress of magnetorheological fluids using the parallel-plate measuring system, Rheol. Acta, 2009, **48**, 89-95.
37. B Rabinowitsch, The viscosity and elasticity of sols, Z Phys Chem, 1929, **1**, 26–145.
38. PR Soskey, HH Winter, Large step shear strain experiments with parallel-disk rotational rheometers. J Rheol, 1984, **28**, 625–645.
39. TG Mezger, The rheology handbook, Vincentz Network, Germany, 2002.
40. WH Li, H Du, G Chen, SH Yeo Experimental investigation of creep and recovery behaviors of magnetorheological fluids. Materials Science and Engineering A, 2002, **333**, 368-376.
41. GM Kamath, NM Wereley, A nonlinear viscoelastic-plastic model for electrorheological fluids, Smart Materials and Structures, 1997, **6,** 351-359.
42. F Gandhi, WA Bullough, On the Phenomenological Modeling of Electrorheological and Magnetorheological Fluid Preyield Behaviour, Journal of Intelligent Material Systems and Structures, 2005, **16,** 237-248.

43. A Zubarev, L Iskakova, P Kuzhir, G Bossis On the theory of magnetoviscous effect in magnetorheological suspensions, Journal of Rheology, 2014, **58**, 1673-1692.
44. D J Klingenberg, J C Ulicny, M A Golden Mason numbers for magnetorheology, J. of Rheology, 2007, **51**, 883-893.
45. J A Ruiz-López, J A Fernández-Toledano, R Hidalgo-Alvarez, J De Vicente, Testing the mean magnetization approximation, dimensionless and scaling numbers in magnetorheology, Soft Matter, 2016, **12**, 1468-1476.
46. FF Fang, HJ Choi, MS Jhon, Magnetorheology of soft magnetic carbonyl iron suspension with single-walled carbon nanotube additive and its yield stress scaling function, Coll. and Surf. A: Physicochem. Eng. Aspects 2009, **351**, 46-51.
47. FF Fang, YD Liu, HJ Choi, Y Seo, Core-shell structured carbonyl iron microspheres prepared via dual-step functionality coatings and their magnetorheological response, ACS App. Mat. & Interfaces 2011, **3**, 3487-3495.
48. J S An, W J Han, H J Choi, Synthesis of hollow magnetite nanoparticles via self-assembly and their magnetorheological properties, Coll. & Surf. A, 2017, **535**, 16-23.
49. D Lambrick, N Mason, N Harris, G Russell, S Hoon, M Kilner, An Iron-cobalt 'alloy' magnetic fluid, IEEE Transactions on Magnetics, 21, 1985, 1891-1893.
50. Injamamul Arief, PK Mukhopadhyay, Preparation of spherical and cubic Fe55Co45 microstructures for studying the role of particle morphology in magnetorheological suspensions, Journal of Magnetism and Magnetic Materials, 360, 2014, 104-108.
51. IG Kim, KH Song, BO Park, BI Choi, HJ Choi, Nano-sized Fe soft-magnetic particle and its magnetorheology, Colloid Polym. Sci., 2011, **289**: 79–83.
52. WJ Han, SH Piao, HJ Choi, Y Seo, Core-shell structured mesoporous magnetic nanoparticles and their magnetorheological response. Colloids and Surfaces A, 2017, **524**: 79-86.
53. W Zhu, X Dong, H Huang, M Qi, Iron nanoparticles-based magnetorheological fluids: a balance between MR effect and sedimentation stability, Jour. Magn. Magn. Materials, 2019, **491**, 165556.
54. G Wang, F Zhou, Z Lu, Y Ma, X Li, Y Tong, X Dong, Controlled synthesis of CoFe2O4/MoS2 nanocomposites with excellent sedimentation stability for magnetorheological fluid, Journal of Industrial and Engineering Chemistry, 2019, **70**: 439-446.